

REIONIZATION OF THE UNIVERSE AND THE PHOTOEVAPORATION OF COSMOLOGICAL MINIHALOS

Paul R. Shapiro

Department of Astronomy, The University of Texas at Austin, USA

and

Alejandro C. Raga

Instituto de Astronomía, Universidad Nacional Autónoma de México

RESUMEN

Las primeras fuentes de radiación ionizante que se condensaron del IGM generaron frentes de ionización en sus alrededores, que iluminaron a otros objetos condensados y los fotoevaporaron. Mostramos la retroalimentación causada por la reionización del Universo en la formación de estructuras cósmicas para el caso de un mini halo de materia oscura y bariones, ionizado por una fuente externa con un espectro similar al de los cuásares, justo después del paso del frente de ionización generado por la fuente. El mini halo es modelado, siguiendo su condensación del gas en expansión así como su virialización, como una esfera isotérmica en equilibrio hidrostático. Se presentan los resultados de la primera simulación hidrodinámica del proceso incluyendo transferencia radiativa. También se dan ejemplos de diagnósticos observacionales, incluyendo la distribución espacial del grado de ionización en el flujo de C, N y O si existen trazas de estos elementos en la densidad columnar integrada de H I, He I y II, así como el C IV a diferentes velocidades en el gas fotoevaporado, que podría ser observado en absorción en contra de la fuente de ionización.

ABSTRACT

The first sources of ionizing radiation to condense out of the dark and neutral IGM sent ionization fronts sweeping outward through their surroundings, overtaking other condensed objects and photoevaporating them. This feedback effect of universal reionization on cosmic structure formation is demonstrated here for the case of a cosmological minihalo of dark matter and baryons exposed to an external source of ionizing radiation with a quasar-like spectrum, just after the passage of the global ionization front created by the source. We model the pre-ionization minihalo as a truncated, nonsingular isothermal sphere in hydrostatic equilibrium following its collapse out of the expanding background universe and virialization. Results are presented of the first gas dynamical simulations of this process, including radiative transfer. A sample of observational diagnostics is also presented, including the spatially-varying ionization levels of C, N, and O in the flow if a trace of heavy elements is present and the integrated column densities of H I, He I and II, and C IV thru the photoevaporating gas at different velocities which would be measured in absorption against a background source like that responsible for the ionization.

Key Words: **COSMOLOGY: THEORY — GALAXIES: FORMATION — HYDRODYNAMICS — INTERGALACTIC MEDIUM**

1. INTRODUCTION

Observations of quasar absorption spectra indicate that the universe was reionized prior to redshift $z = 5$. Recent detections of H Lyman alpha emission lines from sources at even higher redshift ($z \leq 5.6$) strengthen this conclusion (Hu, Cowie, & McMahon 1998; Weymann et al. 1998). As new discoveries push the observable horizon back in time ever-closer to the epoch of reionization at redshift $z > 5$, increased awareness of its importance as a missing link in the theory of galaxy formation has caused a great renewal of interest in universal reionization. If reionization took place early enough, then Thompson scattering of cosmic microwave background (CMB) photons by free electrons in an ionized intergalactic medium (IGM) would also have left a detectable imprint on the CMB observed today. Recent data on the first Doppler peak in the angular spectrum of CMB anisotropy set limits which imply a reionization redshift $z \lesssim 40$ (model-dependent) (Griffiths, Barbosa, & Liddle 1998). (For a review and references on reionization work prior to 1996, the reader is referred to Shapiro 1995, while more recent developments are summarized in Haiman & Knox 1999.)

A review of the theory of reionization is outside the scope of this brief report. In keeping with the focus of this meeting, I will confine myself to a description of some recent progress on the calculational side of the problem. To solve the full reionization problem we must also solve the problem of how density fluctuations led to galaxy formation and this, in turn, led to secondary energy release in the form of ionizing and dissociating radiation by the stars and quasars formed inside early galaxies, as well as other forms of energy release like supernova explosions, jets and winds, which in turn influenced the future course of galaxy formation. The modern context for this description is the Cold Dark Matter (CDM) model, in which a cold, pressure-free, collisionless gas of dark matter dominates the matter density and structure arises from the gravitational amplification of a scale-free power-spectrum of initially small-amplitude, Gaussian-random-noise primordial density fluctuations, in a hierarchical fashion, with small mass objects collapsing out first and merging together to form larger-mass objects which form later. The calculation of these effects poses an enormous multi-scale computational challenge, involving numerical gas dynamics coupled to gravitational N-body dynamics, which raises the bar of cosmological simulation considerably by adding the requirement that radiative transfer effects be included, as well. To simplify matters, I will henceforth focus on just one of the central challenges of reionization theory, the effect of cosmological ionization fronts.

2. IONIZATION FRONTS IN THE IGM

The neutral, opaque IGM out of which the first bound objects condensed was dramatically reheated and reionized at some time between a redshift $z \approx 50$ and $z \approx 5$ by the radiation released by some of these objects. An early analysis of the inhomogeneous nature of reionization for the case of short-lived quasars occurring at random positions in a uniform IGM was described by Arons & Wingert (1972). In that treatment it was assumed that each quasar was instantaneously surrounded by an isolated H II region, a “relict H II region” undergoing recombination only, each such region filling a volume containing just as many initially neutral H atoms as there were ionizing photons emitted by the QSO during its lifetime. The effect of successive generations of QSO’s was accounted for on a statistically-averaged basis by allowing new generations of QSO’s to turn on at random positions, including those inside pre-existing relict H II regions before their H atoms had fully recombined, leading eventually to the complete overlap of these discrete ionized zones.

When the first sources turned on, they actually ionized their surroundings, not instantaneously, but rather by propagating weak, R-type ionization fronts which moved outward supersonically with respect to both the neutral gas ahead of and the ionized gas behind the front, racing ahead of the hydrodynamical response of the IGM, as first described by Shapiro (1986) and Shapiro & Giroux (1987). These authors solved the problem of the time-varying radius of a spherical I-front which surrounds isolated sources in a cosmologically-expanding IGM analytically, taking proper account of the I-front jump condition generalized to cosmological conditions. They applied these solutions to determine when the I-fronts surrounding isolated sources would grow to overlap and, thereby, complete the reionization of the universe (Donahue & Shull 1987 and Meiksen & Madau 1993 subsequently adopted a similar approach to answer that question). The effect of density inhomogeneity on the rate of I-front propagation was described by a mean “clumping factor” $c_l > 1$, which slowed the I-fronts by increasing the average recombination rate per H atom inside clumps. This suffices to describe the rate of I-front propagation as long as the clumps are either not self-shielding or, if so, only absorb a fraction of

the ionizing photons emitted by the central source. Numerical radiative transfer methods are currently under development to solve this problem in 3D for the inhomogeneous density distribution which arises as cosmic structure forms, so far limited to a fixed density field without gas dynamics (e.g. Abel, Norman, & Madau 1999; Razoumov & Scott 1999). The question of what dynamical effect the I-front had on the density inhomogeneity it encountered, however, requires further analysis.

The answer depends on the size and density of the clumps overtaken by the I-front. The fate of linear density fluctuations depends upon their Jeans number, $L_J \equiv \lambda/\lambda_J$, the wavelength in units of the baryon Jeans length in the IGM at temperatures of order 10^4K . Fluctuations with $L_J < 1$ find their growth halted and reversed (cf. Shapiro, Giroux, & Babul 1994). For nonlinear density fluctuations, however, the answer is more complicated, depending upon at least three dimensionless parameters, their internal Jeans number, $L_J \equiv R_c/\lambda_J$, the ratio of the cloud radius R_c to the Jeans length λ_J inside the cloud at about 10^4K , their “Strömgren number” $L_s \equiv 2R_c/\ell_s$, the ratio of the cloud diameter $2R_c$ to the Strömgren length ℓ_s inside the cloud (the length of a column of gas within which the unshielded arrival rate of ionizing photons just balances the total recombination rate), and their optical depth to H ionizing photons at 13.6 eV, τ_H , before ionization. If $\tau_H < 1$, the I-front sweeps across the cloud, leaving an ionized gas at higher pressure than its surroundings, and exits before any mass motion occurs in response, causing the cloud to blow apart. If $\tau_H > 1$ and $L_s > 1$, however, the cloud shields itself against ionizing photons, trapping the I-front which enters the cloud, causing it to decelerate inside the cloud to the sound speed of the ionized gas before it can exit the other side, thereby transforming itself into a weak, D-type front preceded by a shock. Typically, the side facing the source expels a supersonic wind backwards towards the source, which shocks the IGM outside the cloud, while the remaining neutral cloud material is accelerated away from the source by the so-called “rocket effect” as the cloud photoevaporates (cf. Spitzer 1978). As long as $L_J < 1$ (the case for gas bound to dark halos with virial velocity less than 10 km s^{-1}), this photoevaporation proceeds unimpeded by gravity. For halos with higher virial velocity, however, $L_J > 1$, and gravity competes with pressure forces. For a uniform gas of H density $n_{\text{H,c}}$, located a distance r_{Mpc} (in Mpc) from a UV source emitting $N_{\text{ph},56}$ ionizing photons (in units of 10^{56}s^{-1}), the Strömgren length is only $\ell_s \cong (100\text{ pc})(N_{\text{ph},56}/r_{\text{Mpc}}^2)(n_{\text{H,c}}/0.1\text{ cm}^{-3})^{-2}$. We focus in what follows on the self-shielded case which traps the I-front.

3. THE PHOTOEVAPORATION OF DWARF GALAXY MINIHALOS OVERTAKEN BY A COSMOLOGICAL IONIZATION FRONT

The importance of this photoevaporation process has long been recognized in the study of interstellar clouds exposed to ionizing starlight (e.g. Oort & Spitzer 1955; Spitzer 1978; Bertoldi 1989; Bertoldi & McKee 1990; Lefloch & Lazareff 1994; Lizano et al. 1996). Radiation-hydrodynamical simulations were performed in 2D in the early 1980’s of a stellar I-front overtaking a clump inside a molecular cloud (Sandford, Whitaker, & Klein 1982; Klein, Sandford, & Whitaker 1983). More recently, 2D simulations for the case of circumstellar clouds ionized by a single nearby star have also been performed (Mellema et al. 1998). In the cosmological context, however, the importance of this process has only recently been fully appreciated. In proposing the expanding minihalo model to explain Lyman alpha forest (“LF”) quasar absorption lines, Bond, Szalay, & Silk (1988) discussed how gas originally confined by the gravity of dark minihalos in the CDM model would be expelled by pressure forces if photoionization by ionizing background radiation suddenly heated all the gas to an isothermal condition at $T \approx 10^4\text{K}$. The first radiation-hydrodynamical simulations of the photoevaporation of a primordial density inhomogeneity overtaken by a cosmological I-front, however, were described in Shapiro, Raga, & Mellema (1997, 1998). Barkana & Loeb (1999) subsequently considered the relative importance of this process for dwarf galaxy minihalos of different masses in the CDM model, using static models of uniformly-illuminated spherical clouds in thermal and ionization equilibrium, taking H atom self-shielding into account, and assuming that gas which is heated above the minihalo virial temperature must be evaporated. They concluded that 50%–90% of the gas in gravitationally bound objects when reionization occurred should have been evaporated.

As a first study of these important effects, Shapiro, Raga, & Mellema (1997, 1998) simulated the photoevaporation of a uniform, spherical, neutral, intergalactic cloud of gas mass $1.5 \times 10^6 M_\odot$, radius $R_c = 0.5\text{ kpc}$, density $n_{\text{H,c}} = 0.1\text{ cm}^{-3}$ and $T = 100\text{ K}$, located 1 Mpc from a quasar with emission spectrum $F_\nu \propto \nu^{-1.8}$ ($\nu > \nu_{\text{H}}$) and $N_{\text{ph}} = 10^{56}\text{s}^{-1}$, initially in pressure balance with an ambient IGM of density 0.001 cm^{-3} which

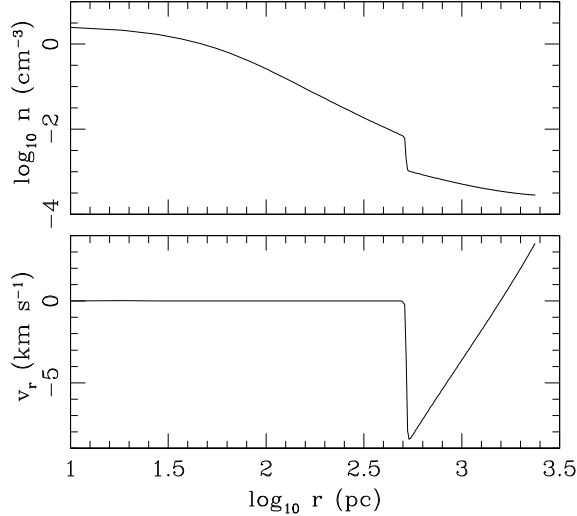


Figure 1. MINIHALO INITIAL CONDITIONS BEFORE REIONIZATION: Truncated, nonsingular isothermal sphere (TIS) of gas and dark matter in hydrostatic equilibrium (Shapiro, Iliev, & Raga 1999) surrounded by the corresponding self-similar spherical infall for an Einstein-de Sitter background universe (cf. Bertschinger 1985). (a) (Top) gas density and (b) (Bottom) gas velocity versus distance from minihalo center.

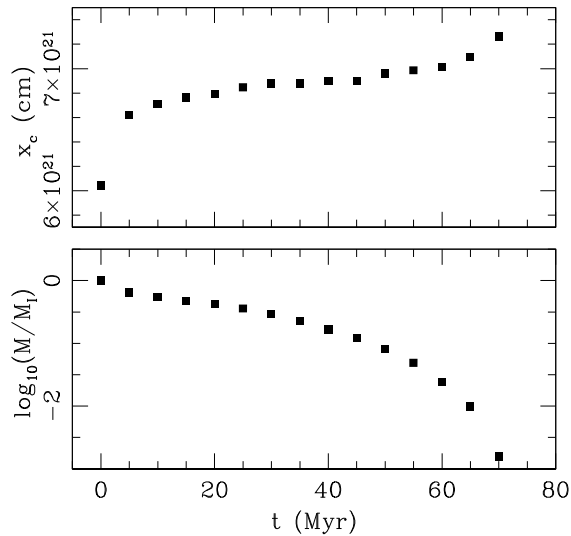


Figure 2. IONIZATION FRONT PHOTOEVAPORATES MINIHALO: (a) (Top) I-front position along x -axis versus time; (b) (Bottom) Mass fraction of the initial mass M_I of minihalo hydrostatic core which remains neutral (H I) versus time.

at time $t = 0$ had just been photoionized by the passage of the intergalactic R-type I-front generated when the quasar turned on [i.e. $(L_J, L_s, \tau_H) \approx (0.1, 10, 10^3)$]. [A standard top-hat perturbation which collapses and virializes at $z_{\text{coll}} = 9$, for example, with total mass $\cong 10^7 M_\odot$, has circular velocity $v_c \cong 7 \text{ km s}^{-1}$, $R_c \cong 560 \text{ pc}$, and $n_{\text{H,c}} = 0.1 \text{ cm}^{-3}$, if $\Omega_{\text{bary}} h^2 = 0.03$ and $h = 0.5$.] The cloud contained H, He, and heavy elements at 10^{-3} times the solar abundance. Our simulations in 2D, axisymmetry used an Eulerian hydro code with Adaptive Mesh Refinement and the Van Leer flux-splitting algorithm, which solved nonequilibrium ionization rate equations (for H, He, C, N, O, Ne, and S) and included an explicit treatment of radiative transfer by taking into account the bound-free opacity of H and He (Raga et al. 1995; Mellema et al. 1997; Raga, Mellema, & Lundquist 1997). The reader is referred to Shapiro et al. (1997, 1998) for further details.

Here we shall present for the first time the results of simulations of a more realistic, cosmological minihalo, in which the uniform cloud described above is replaced by a self-gravitating, centrally condensed object. Our initial condition before ionization, shown in Figure 1, is that of a $10^7 M_\odot$ minihalo in an Einstein-de Sitter universe ($\Omega_{\text{CDM}} = 1 - \Omega_{\text{bary}}$; $\Omega_{\text{bary}} h^2 = 0.02$; $h = 0.7$) which collapses out and virializes at $z_{\text{coll}} = 9$, yielding a truncated, nonsingular isothermal sphere of radius $R_c = 0.5 \text{ kpc}$ in hydrostatic equilibrium with virial temperature $T_{\text{vir}} = 5900 \text{ K}$ and dark matter velocity dispersion $\sigma = 6.3 \text{ km s}^{-1}$, according to the solution of Shapiro, Iliev, & Raga (1999), for which the finite central density inside a radius about $1/30$ of the total size of the sphere is 514 times the surface density. This hydrostatic core of radius R_c is embedded in a self-similar, spherical, cosmological infall according to Bertschinger (1985). The results of our simulation on an (r, x) -grid

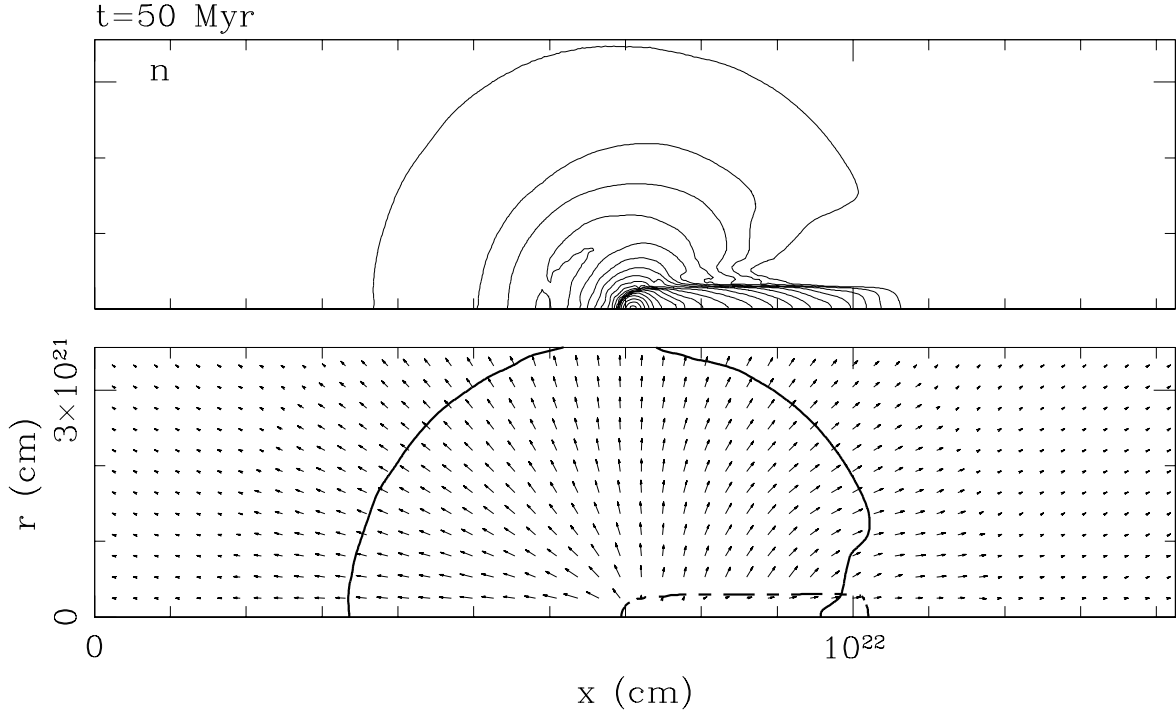


Figure 3. PHOTOEVAPORATING MINIHALO. 50 Myr after turn-on of quasar 1 Mpc to the left of computational box along the x -axis. (a) (Upper Panel) isocontours of atomic density, logarithmically spaced, in (r, x) -plane of cylindrical coordinates; (b) (Lower Panel) velocity arrows are plotted with length proportional to gas velocity. An arrow of length equal to the spacing between arrows has velocity 30 km s^{-1} . Solid line shows current extent of gas originally in hydrostatic core. Dashed line is I-front (50% H-ionization contour).

with 256×512 cells (fully refined) are summarized in Figures 2–6. The background IGM and infalling gas outside the minihalo are quickly ionized, and the resulting pressure gradient in the infall region converts the infall into an outflow. The I-front is trapped, however, inside the hydrostatic core of the minihalo. Figure 2(a) shows the position of the I-front inside the minihalo as it slows from weak, R-type to weak D-type as it advances across the original hydrostatic core. Figure 2(b) shows the mass of the neutral zone within the original hydrostatic core shrinking as the minihalo photoevaporates within about 70 Myrs. This photoevaporation time is significantly less than that found previously for a similar-mass object with the same external source in the uniform cloud case. Figures 3 and 4 show the structure of the photoevaporative flow 50 Myrs after the global I-front first overtakes the minihalo, with key features of the flow indicated by the labels on the temperature plot in Figure 4. Figure 5 shows the spatial variation of the relative ionic abundances of C, N, O ions along the symmetry axis after 50 Myrs. As in the case of the uniform cloud, Figure 5 shows the presence at 50 Myrs of low as well as high ionization stages of the metals. Compared to the uniform cloud case at the same time-slice, however, Figure 5 shows a somewhat higher degree of ionization on the side facing the source than in those previous results. The column densities of H I, He I and II, and C IV for minihalo gas of different velocities as seen along the symmetry axis at different times are shown in Figure 6. At early times, the cloud gas resembles a weak Damped Lyman Alpha (“DLA”) absorber with small velocity width ($\sim 10 \text{ km s}^{-1}$) and $N_{\text{HI}} \sim 10^{20} \text{ cm}^{-2}$, with a LF-like red wing (velocity width $\sim 10 \text{ km s}^{-1}$) with $N_{\text{HI}} \sim 10^{16} \text{ cm}^{-2}$ on the side moving toward the quasar, with a C IV feature with $N_{\text{CIV}} \sim 10^{12} \text{ cm}^{-2}$ displaced in this same asymmetric way from the velocity of peak H I column density. After 160 Myr, however, only a narrow H I feature with LF-like column density $N_{\text{HI}} \sim 10^{14} \text{ cm}^{-2}$ remains, with $N_{\text{HeII}}/N_{\text{HI}} \sim 10^2$ and $N_{\text{CIV}}/N_{\text{HI}} \sim [\text{C}]/[\text{C}]_{\odot}$. A comparison with the results of

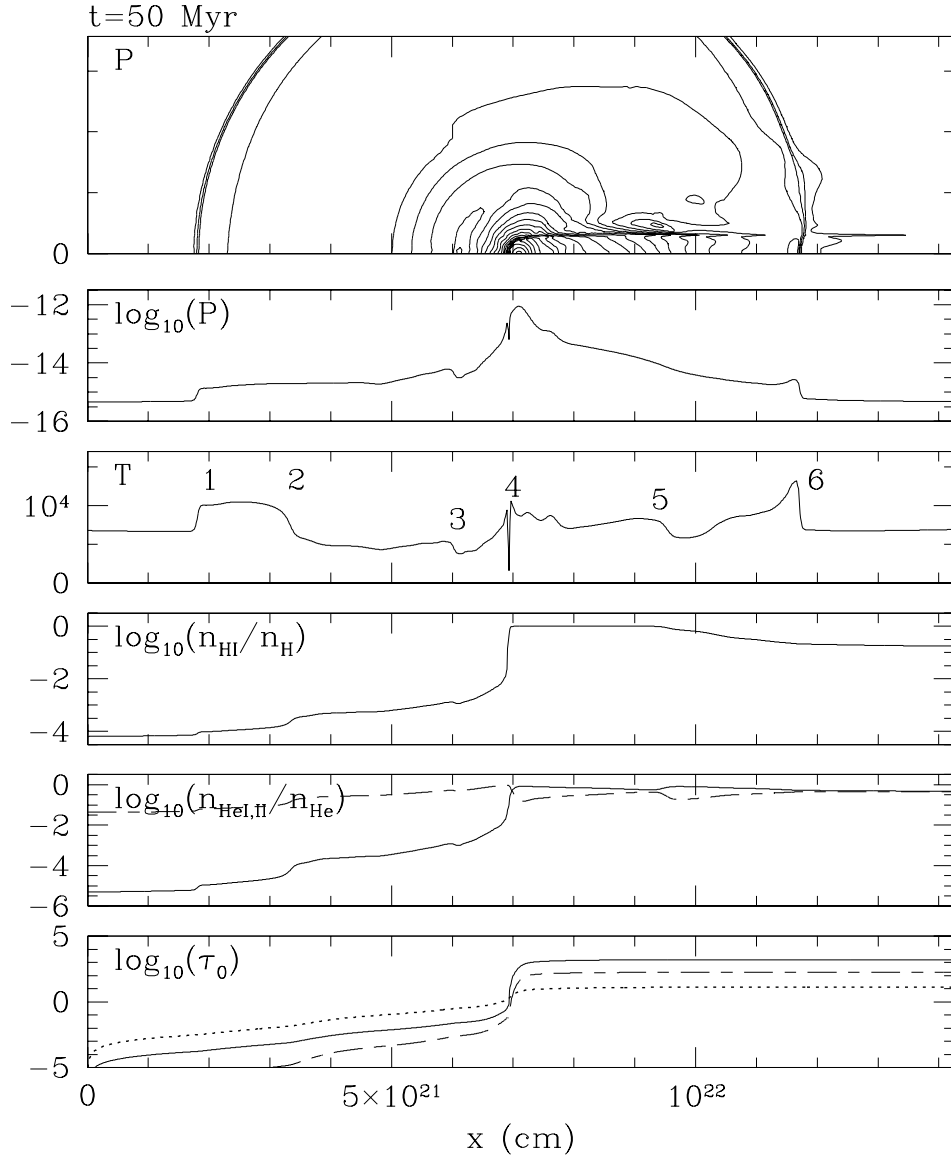


Figure 4. PHOTOEVAPORATING MINIHALO. One time-slice 50 Myr after turn-on of quasar located 1 Mpc away from cloud to the left of computational box along the x -axis. From top to bottom: (a) isocontours of pressure, logarithmically spaced, in (r, x) -plane of cylindrical coordinates; (b) pressure along the $r = 0$ symmetry axis; (c) temperature; (d) H I fraction; (e) He I (solid) and He II (dashed) fractions; (f) bound-free optical depth along $r = 0$ axis at the threshold ionization energies for H I (solid), He I (dashed), He II (dotted). Key features of the flow are indicated by the numbers which label them on the temperature plot: 1 = IGM shock; 2 = contact discontinuity between shocked cloud wind and swept up IGM; 3 = wind shock; between 3 and 4 = supersonic wind; 4 = I-front; 5 = boundary of gas originally in hydrostatic core; 6 = shock in shadow region caused by compression of shadow gas by shock-heated gas outside shadow.

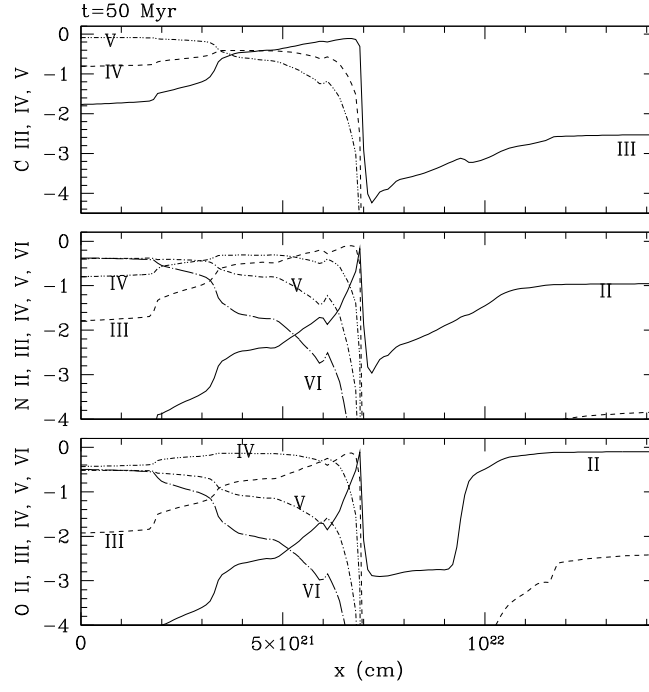


Figure 5. OBSERVATIONAL DIAGNOSTICS OF PHOTOEVAPORATING MINIHALO I: IONIZATION STRUCTURE OF METALS. Carbon, nitrogen, and oxygen ionic fractions along symmetry axis at $t = 50$ Myr.

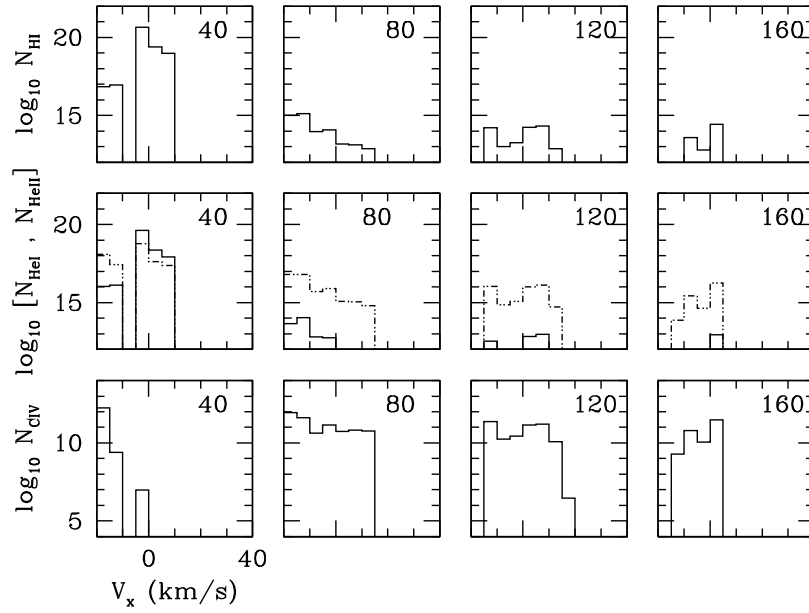


Figure 6. OBSERVATIONAL DIAGNOSTICS OF PHOTOEVAPORATING MINIHALO II. ABSORPTION LINES: Cloud column densities (cm^{-2}) along symmetry axis at different velocities. (Top) H I; (Middle) He I (solid) and He II (dotted); (Bottom) C IV. Each box labelled with time (in Myrs) since QSO turn-on.

the uniform cloud case in Shapiro et al. (1997, 1998) shows that, despite their differences, there is a surprising degree of similarity between the qualitative features presented there and those found here for a highly centrally-concentrated minihalo. Future work will extend this study to minihalos of higher virial temperatures, for which gravity competes more effectively with photoevaporation.

This work was supported by NASA Grants NAG5-2785, NAG5-7363, and NAG5-7821, and NSF Grant ASC-9504046, and was made possible by a UT Dean's Fellowship and a National Chair of Excellence, UNAM, México awarded by CONACyT in 1997 to Shapiro. This material is based in part upon work supported by the Texas Advanced Research Program under Grant No. 3658-0624-1999.

REFERENCES

- Abel, T., Norman, M. L., & Madau, P. 1999, *ApJ*, 523, 66
- Arons, J., & Wingert, D. W. 1972, *ApJ*, 177, 1
- Barkana, R., & Loeb, A. 1999, *ApJ*, 523, 54
- Bertoldi, F. 1989, *ApJ*, 346, 735
- Bertoldi, F., & McKee, C. 1990, *ApJ*, 354, 529
- Bertschinger, E. 1985, *ApJS*, 58, 39
- Bond, J. R., Szalay, A. S., & Silk, J. 1988, *ApJ*, 324, 627
- Donahue, M., & Shull, J. M. 1987, *ApJ*, 323, L13
- Griffiths, L. M., Barbosa, D., & Liddle, A. R. 1998, *MNRAS*, 308, 854
- Haiman, Z., & Knox, L. 1999, in *ASP Conf. Ser. Vol. 181, Sloan Summit on Microwave Foreground*, ed. A. de Oliveira & M. Tegmark (San Francisco: Astronomical Society of the Pacific), 227 (astro-ph/9902311)
- Hu, E. M., Cowie, L. L., & McMahon, R. G. 1998, *ApJ*, 502, 99
- Klein, R. I., Sandford, M. T., & Whitaker, R. W. 1983, *ApJ*, 271, L69
- Lefloch, B., & Lazareff, B. 1994, *A&A*, 289, 559
- Lizano, S., Cantó, J., Garay, G., & Hollenbach, D. 1996, *ApJ*, 468, 739
- Meiksen, A., & Madau, P. 1993, *ApJ*, 412, 34
- Mellema, G., Raga, A. C., Canto, J., Lundqvist, P., Balick, B., Steffen, W., & Noriega-Crespo, A. 1998, *A&A*, 331, 335
- Oort, J. H., & Spitzer, L. 1955, *ApJ*, 121, 6
- Raga, A. C., Taylor, S. D., Cabrit, S., & Biro, S. 1995, *A.A.*, 296, 833
- Raga, A. C., Mellema, G., & Lundquist, P. 1997, *ApJS*, 109, 517
- Razoumov, A., & Scott, D. 1999, *MNRAS*, 309, 287
- Sandford, M. T., Whitaker, R. W., & Klein, R. I. 1982, *ApJ*, 260, 183
- Shapiro, P. R. 1995, in *ASP Conf. Ser. Vol. 80, The Physics of the Interstellar Medium and The Intergalactic Medium*, ed. A. Ferrara, C. F. McKee, C. Heiles, & P. R. Shapiro (San Francisco: Astronomical Society of the Pacific), 55
- Shapiro, P. R. 1986, *PASP*, 98, 1014
- Shapiro, P. R., & Giroux, M. L. 1987, *ApJ*, 321, L107
- Shapiro, P. R., Giroux, M. L., & Babul, A. 1994, *ApJ*, 427, 25
- Shapiro, P. R., Iliev, I. T., & Raga, A. C. 1999, *MNRAS*, 307, 203
- Shapiro, P. R., Raga, A. C., & Mellema, G. 1997, in *Structure and Evolution of the Intergalactic Medium From QSO Absorption Line Systems*, ed. P. Petitjean & S. Charlot (Gif-sur-Yvette: Editions Frontières), 41
- Shapiro, P. R., Raga, A. C., & Mellema, G. 1998, in *Mem. Soc. Astron. Italiana Vol. 69, H₂ in the Early Universe*, ed. E. Corbelli, D. Galli, & F. Palla, 463 (astro-ph/9804117)
- Spitzer, L. 1978, *Physical Processes in the Interstellar Medium* (New York: Wiley Interscience)
- Weymann, R. J., Stern, D., Bunker, A., Spinrad, H., Chaffee, F. H., Thompson, R. I., & Storrie-Lombardi, L. J. 1998, *ApJ*, 505, L95

P. R. Shapiro: Department of Astronomy, University of Texas, Austin, TX 78712, USA (shapiro@astro.as.utexas.edu)

A. C. Raga: Instituto de Astronomía, UNAM, Apartado Postal 70-264, 04510 México D. F., México (raga@astroscu.unam.mx)